Journal of the Technical University of Gabrovo

https://mc04.manuscriptcentral.com/jtug

INCREASING THE EFFICIENCY OF DIAMOND DRILLING OF CARBON COMPOSITES BY A DEVICE WITH COMBINED ELECTRIC MACHINES

Oleksandr Salenko[1*], Olga Chencheva[2], Viktor Shchetynin[2], Valentina Gluchova[2], Lashko Evgeny[2], Mohamed Budar[2]

[1]*National technical University of Ukraine „Igor Sikorsky Kyiv Polytechnic Institute", Kyiv, Ukraine*

[2]*Kremenchuk Mykhailo Ostrohradskyi National University, Kremenchuk, Ukraine*

ARTICLE INFO

Article history:
Received 15 January 2020
Accepted 31 March 2020

Keywords:
carbon composites, drilling, mechanics of composite materials, combined electrical machines.

ABSTRACT

The paper presents an original solution to the actual problem of increasing the efficiency of the drilling of composite materials of the carbonic group through the use of coupled electric rotary type machines whose combination of movements allows to obtain controlled rotary-reciprocating motion of the instrument. Show, by creating cyclic low frequency load of the cutting zone, it is possible to improve the efficiency and quality of processing, without destroying the composite. Stress state of the cutting zone in composite materials based on carbon fibers has been evaluated and it is proved that their processing with ring diamond-coated drills is reasonable and effective. The use of a cyclic linear feeder allows significantly reducing the thickness of the destructive layer and reducing the cutting force, requiring further research on the issue of rational geometric dimensions of the tool end, the presence of cavity elements on it to remove the microstrip from the processing area.

It is also proven that the proposed design of a power head with coupled electric machines to provide rotary and translatory motion in coaxial execution is a promising technical solution that can be successfully implemented in both manual tools and automated processing programmed control systems.

© 2020 Journal of the Technical University of Gabrovo. All rights reserved.

1. INTRODUCTION

Actuality of the work. In modern mechanical engineering, new composite materials with predetermined physical and mechanical properties are becoming more widespread, among which the fiber-laminated composite based on glass and graphite fibers account for greatest number. Such materials are characterized by an entire complex of physical and mechanical properties demanded by high-tech production: strength, anisotropy, satisfactory heat resistance, low weight, high load capacity, etc.

The advantages in weight while maintaining directional strength and elasticity (see table 1, [1]) makes such materials the most promising in aviation and rocket science.

Table 1 *Properties of some structural materials comparing with some metals*

Material	Density, kg/m^3	Tensile strength, MPa	Young's modulus, GPa	Specific Strength, E ·10^3, km	Specific module, E·10^6, km
Carbon fiber	1450-1600	780-1800	120-130	5-112	9-25
Fiberglass	2120	1926	69	91	3,2
High strength steel	7806	1402	210	18	2,7
Aluminium alloy	2710	503	75	18	2,7
Titanium alloy	4430	1002	110	28	2,5
Polyamide 6.6	1140	82,6	28	7,24	0,24

Despite the fact that most of the products can be given the necessary shape at the stage of the workpiece pre-shaping, the need for finishing and bringing to the technical requirements is still relevant. Thus, the execution of different openings, ledges, window punching, edge processing – usually accompany any technological process and sometimes exceed the layout, saturation with adhesive, and shaping of the product as a whole. Another problem is the heterogeneous structure of the material and the sharp difference in the mechanical properties of its components, which ultimately leads to a sharp deterioration of the edge quality when trying to processing similar materials with a traditional cutting tool.

That is why finding methods and ways to improve the efficiency of processing, ensuring its proper quality is the main focus of research by processing leading experts.

The most difficult to perform are holes that are difficult to form in the preliminary stages. Only mechanical or

* Corresponding author. E-mail: salenko2006@ukr.net

advanced-technical finish processing [2] is able to provide the required accuracy of such elements, dimensional stability and good quality of the surface layer. Despite the wide variety of tool designs for making holes, [3] traditionally, holes in composite products are made with diamond-coated tubular drills. Typical designs of such drills are presented in table 2, [4].

Table 2 *Some examples of design the drill middle diameters*

№	Design	Parameters	Appointment
1	The drill is tubular 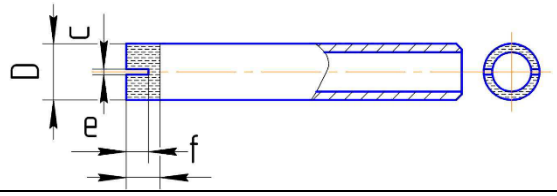	*D* =4…12 мм; *c*, *e* – width and depth of two grooves; *f* is the length of the layer. Grit: 125/100	Drilling holes diameter from 4.0 up to 12.0 mm
2	The drill is annular 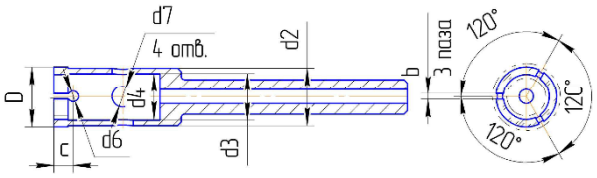	*D* =14…24 мм; *c* – depth of finding holes; *d*6; *b* - width market; *d*2, *d*3, *d*4, *d*7 – the size of the constructing elements. Grit: 160/125	Drilling holes diameter from 12,0 up to 24,0 мм

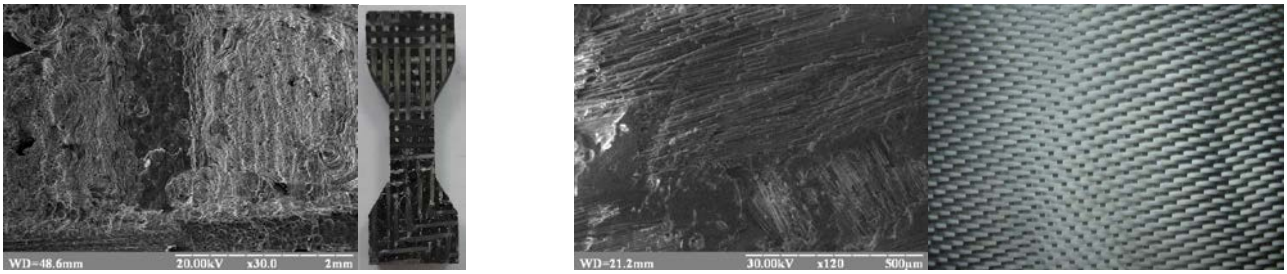

a) *b)*

Fig. 1. Microstructure of carbon-carbon material (a) and carbon plastic (b)

The fundamental difference between the structure of the material and metals, the physico-mechanical properties of its components, forces researchers to focus on the features of the cutting / micro-cutting process, the material in order to obtain the correct geometric shapes and maintain the quality of the surface layer at the required level. The possibility of delamination, damage to the adhesive contact has been studied in many works, in particular, [5], [6], [7]. Studying the heat in the cutting zone, the authors of [8] concluded that this parameter is important, especially for polymer-based materials. Moreover, it was shown in [9] that during grinding, the diamond surface layer heats up to critical temperatures. The authors of [10], [11], proposing the original design of the drill, made the most important conclusion that lowering the temperature and improving the cutting properties during processing of composites is possible due to interrupted cutting.

RESEARCH METHOD

The processed composites are a heterogeneous structure, the components of which are fundamentally different in mechanical properties. Reinforced with reinforcing fibers with a diameter of 3 ... 5 microns (sometimes organized into bundles), Fig. 1a, the polymer matrix exhibits properties that complicate the removal of chips from the surface of the material due to the occurrence of adhesion, chemical reactions, high-intensity abrasive wear, and localization of heat on the surface of the cutting wedge. The situation is even more complicated in the case of processing materials of the carbon-carbon group having a porous structure (Fig. 1, b). That is why the behavior of the material is considered the positions of micro- and macromechanics [12].

Micromechanics of the material. Effective processing of composites is achieved in the following ways:

1) by using cutting tools with a special cutting edge profile [11];

2) by creating additional loads in the cutting zone, leading to the redistribution of stresses in the tool area and changing the direction of crack development [12];

3) changing the power load and the direction of movement of the cutting edge by involving activating motions (due to, for example, cyclic or impact feed).

The latter method has the simplest technical implementation, since it does not require the installation of additional mechanical elements or devices bringing additional energy to the area of influence; variable power load may be provided by appropriate movements of the tool itself.

Let’s assume that the surface layer in the processed area is formed by the integrated action of the aggregate of abrasive grains, 3_i which carry out the spatial motion

together with the base (tube) on which they are rigidly fixed (fig. 2).

The trajectory of movement of the latter will be conditioned by simultaneous rotational (P_1) and reciprocating (P_2) motions, and in general will form be segments of a helical line, the length of which corresponds to the presence of a cavity in the body of the composite.

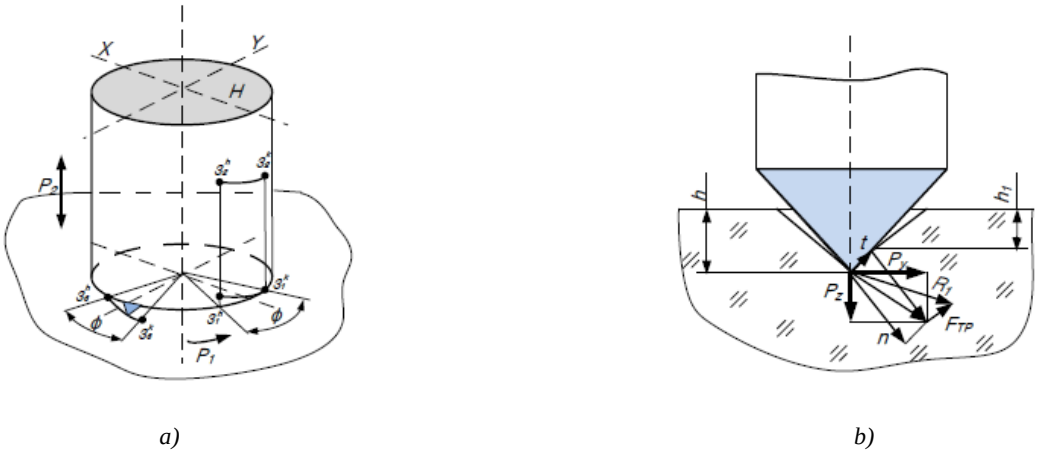

a) *b)*

Fig. 2. Grain movement (a) and scheme of its interaction (b) with the processed surface

The trajectory of grain motion is described by the following system of equations:

$$x = r\sin\varphi$$
$$y = r\cos\varphi, \quad (1)$$
$$z = \frac{s}{n}\varphi$$

where r – the distance from the center of the drill to the considered grain (mm); φ – the angle of the drill rotation; S – feed (mm/min); n – the number of the drill revolutions in min; x, y, z – the grain coordinates.

Let us accept a number of assumptions. Let the cutting surface look like an envelope of micro-grooves, described by the trajectory of grain movement, provided that they are contacted with the medium in the form of a processed half-space.

Because carbon fiber has a number of cavities and caverns, the trajectories of grain movement will be intermittent; on the other hand, the geometric parameters of the tool abrasive layer will also be variable, since during the processing the emerging sludge will partially stick to the surface, altering the grain reach, and the variable cutting forces and high temperature in the interaction zone may cause grains to be broken off in bits.

The work tool forms the lateral and butt surfaces of the cut.

For the butt surface erosion is maximum, since it is determined by the regular feed, and for the lateral surfaces – the minimum, and determines the surface roughness, with minimal fiber breakage.

To determine the length of the interaction line, we use the concept of the primary structural element of the composite (PSE). Let's assume that such an element is a cylindrical body with a diameter d_v, on the surface of which there is a layer s_{pv} of the matrix, and layer s_{pp} of the cavity (fig. 3).

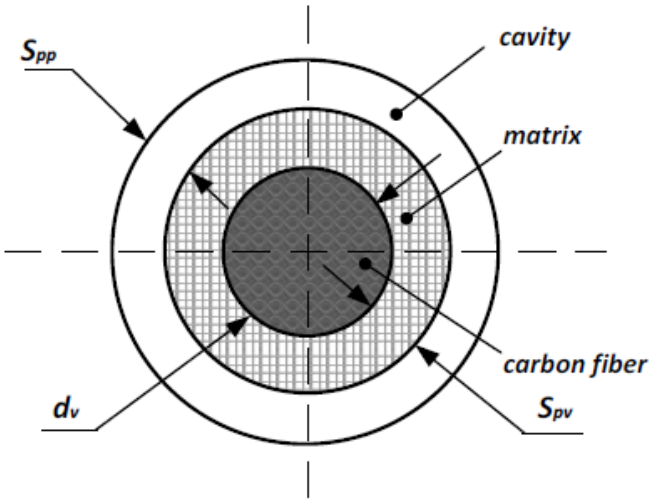

Fig. 3. Primary structural element (PSE) and its geometric characteristics

These layers [5] can be characterized as: a cylindrical body with a diameter d_v consisting of a set of carbon unidirectional fibers, an intermediate layer with a thickness s_{pv} – a polymeric matrix, a layer s_{pp} – a conditionally cavity layer with separate unidirectional oriented fibers.

Taking into accounts that for an infinitesimal parallelepiped of a deformable body, the components of the strain tensor are defined as:

$$\varepsilon_{ij} = \frac{1}{2}\left(\frac{\partial u_i}{\partial v_j} + \frac{\partial u_j}{\partial x_i}\right), i, j = 1,2,3, \quad (2)$$

where u_1, u_2, u_3 – projections of total displacements on the x_1, x_2, x_3 axes, then the Hooke law for an isotropic body will be:

$$\varepsilon_{11} = \frac{1}{E}\left[\sigma_{11} - \mu(\sigma_{22} + \sigma_{33})\right],\ j_{12} = \frac{\sigma_{12}}{G};$$
$$\varepsilon_{22} = \frac{1}{E}\left[\sigma_{22} - \mu(\sigma_{11} + \sigma_{33})\right],\ j_{23} = \frac{\sigma_{23}}{G}; \quad (3)$$
$$\varepsilon_{33} = \frac{1}{E}\left[\sigma_{33} - \mu(\sigma_{22} + \sigma_{11})\right],\ j_{31} = \frac{\sigma_{31}}{G};$$

where E – the material modulus of elasticity; G – the shear modulus; μ – the Poisson's ratio, in this case $G = \frac{E}{2(1+\mu)}$.

In matrix form, Hooke's law will be written as $[\varepsilon] = [\Psi][\sigma]$, $[\Psi]$ – the matrix of malleability, which determines the anisotropy of the properties of the body.

Then for the matrix layers and conditionally cavity layer we obtain:

$$[\Psi]^{spp,spv} = \frac{1}{E}\begin{bmatrix} 1 & -\mu & -\mu & 0 & 0 & 0 \\ -\mu & 1 & -\mu & 0 & 0 & 0 \\ -\mu & -\mu & 1 & 0 & 0 & 0 \\ 0 & 0 & 0 & 2(1+\mu) & 0 & 0 \\ 0 & 0 & 0 & 0 & 2(1+\mu) & 0 \\ 0 & 0 & 0 & 0 & 0 & 2(1+\mu) \end{bmatrix}$$

And for the central nucleus (as orthotropic in the plane of force load action):

$$[\Psi]^{dv} = \frac{1}{E}\begin{bmatrix} \frac{1}{E_1} & \frac{-\mu_{21}}{E_2} & \frac{-\mu_{31}}{E_3} & 0 & 0 & 0 \\ \frac{-\mu_{12}}{E_1} & \frac{1}{E_2} & \frac{-\mu_{32}}{E_3} & 0 & 0 & 0 \\ \frac{-\mu_{13}}{E_1} & \frac{-\mu_{23}}{E_2} & \frac{1}{E_3} & 0 & 0 & 0 \\ 0 & 0 & 0 & 1/G_{12} & 0 & 0 \\ 0 & 0 & 0 & 0 & 1/G_{23} & 0 \\ 0 & 0 & 0 & 0 & 0 & 1/G_{31} \end{bmatrix} \quad (4)$$

Here E_1, E_2, E_3 – modulus of elasticity relative to axes x_1, x_2, x_3 direction; G_1, G_2, G_3 – shear modulus in planes (x_1,x_2), (x_2,x_3), (x_3,x_1), μ_{ij} – Poisson ratios.

In its motion, the abrasive grain interacts with each PSE component. However, the working conditions of single grains on the butt and on the lateral surface are different.

The butt surface (grain 3_3), which can be represented as a discontinuous surface layer at the macro level, with the step of cavities t_p, defined as $t_p = d_v/2 + s_{pp} + s_{vv}$, perceives the load from individual grains according to fig. 2b. Such an interaction can be represented as a jumping deepening of a conical indenter (diamond) under the axial action P_z at the depth h, resulting in a cleavage with a cleavage angle β after which a tangential force is applied P_y. Initially, the indenter slides along the generating line of cone upwards under the action of the constituent t until the time moment when the force P_z is sufficient to destroy the layer having depth h_1. The indenter overcomes the friction force between the chips and the base material. The sliding value of the indenter is determined by the radius of a single grain rounding. The interaction of the diamond grain with the surface of the material being processed at the ratio of depth of penetration h to the radius of curvature of the cutting edge ρ is less than 0,01, is characterized by elastic stamping of the material, that is, the absence of its removal.

Under the action of normal force at the point of contact, the stresses are determined by the corresponding Hertz formulas, which, for the case of contact of the abrasive grain with rounding r_1 and r_2 radius of the rigid component (fiber bundle) according to the PSE concept will be: $\sigma_k = \frac{m_P P_z^{1/3} E^{2/3}}{r^{2/3}}$, where $m = 1 + \frac{r_1}{r_2}$, E – the normalized modulus of elasticity, $E = \frac{2E_1E_2}{E_1 + E_2}$, r – the normalized contact radius, $\frac{1}{r} = \frac{1}{r_1} + \frac{1}{r_2}$.

For grain operating as a peripheral part (for example, 3_1) the contact will occur due to the elastic squeeze of the fiber bundles after contact with the butt and lateral grains (3_3 and 3_2).

Since the fibers strength margin is much higher than the stress created by the working grain, it can be assumed that the fibers that come to the surface and bound to the base matrix, will be destroyed by the mechanism of opening microcracks on the adhesion planes.

Then the moment M_f of the applied external forces to the fibers will be: $M_f = \frac{3l}{2b} M_0 \cos\omega t$.

The load application frequency will be determined by the geometric parameters of the PSE and will be:

$$\omega = \frac{\pi D}{\frac{d_v}{2} + s_{pp} + s_{pv}} n. \quad (5)$$

In this case, the stresses at the base of the crack are determined by the dependence $\sigma = \sigma_k + \left(\frac{b-l}{b}\right)\frac{3M_f}{2b^2}\cos\omega t$, where M_0 – the moment set by the previous equation, b,l – the geometric parameters of the microcrack (fig. 4).

Then we have the value of the stress intensity factor $k = \sigma_k + \left(\frac{b-l}{b}\right)\frac{3M_f}{2b^2}\cos\omega t\sqrt{\pi a}$, a – half the length of the open crack.

The rate of energy release associated with k will be: $G = \frac{1-\nu^2}{E} A(V) k^2$, that under condition of the excess energy released transfer to the (G - R), kinetic energy of the motion of the crack points, it will lead to a rapid increase in the length of the crack $\frac{da}{dN} = \left(\frac{\Delta k}{\bar{c}}\right)^n$.

From the last equation, the maximum crack length a_c is determined by the number of loading cycles N and the initial crack length at its inception a_0:

$$a_c = \frac{a_0}{\sqrt[n/2-1]{1 - \frac{\pi CDnt}{\left(\frac{d_v}{2} + s_{pp} + s_{pv}\right)K}}}, \quad (6)$$

where $C = a_0^{n/2-1}\left(\frac{\sigma}{\rho}\right)^n\left(\frac{\rho}{\bar{c}}\right)^n$, $K = \frac{1}{\sqrt{\pi}(n/2-1)}$, a_0 – the initial crack length; ρ – material density; n, $\bar{c}$ – the material constants; σ – the microstress.

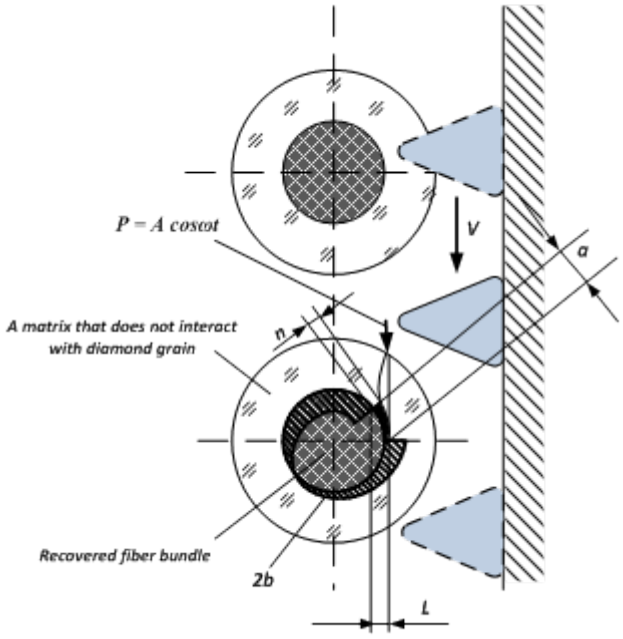

Fig. 4. The effect of a diamond grain on the recovered fiber bundle on the lateral surface of the hole

Macromechanics of the material. Suppose that the drill is a pipe with an outer radius r_z and an inner r_{bn}, the pipe is positioned perpendicular to the surface, and under force impact causes emergence of stresses σ_r, σ_z, σ_t and τ in relevant microvolumes of the body having thickness hob. The body is heterogeneous, with cavities, whose mechanical properties according to the PSE concept is (fig. 3).

The constituents of the displacements $U(t)$ and $H(t)$ at a certain point of the surface, which perceives almost perpendicular loading, according to the design model (fig. 5a), can easily be obtained from the equations connecting stresses and strains:

$$\begin{aligned}
\sigma_r &= 2G\left(\frac{\partial U}{\partial r} + \frac{\mu\varepsilon}{1-2\mu}\right);\\
\sigma_t &= 2G\left(\frac{U}{r} + \frac{\mu\varepsilon}{1-2\mu}\right);\\
\sigma_z &= 2G\left(\frac{\partial H}{\partial z} + \frac{\mu\varepsilon}{1-2\mu}\right);\\
\tau &= G\left(\frac{\partial H}{\partial z} + \frac{\mu\varepsilon}{1-2\mu}\right).
\end{aligned} \tag{7}$$

under condition that:

$$\varepsilon = \varepsilon_r + \varepsilon_t + \varepsilon_z = \frac{\partial U}{\partial r} + \frac{U}{r_m}\frac{\partial H}{\partial z},$$

$$\varepsilon = \frac{1-2\mu}{2(1-\mu)G}(\sigma_r + \sigma_t + \sigma_z) = \frac{1-2\mu}{E}(\sigma_r + \sigma_t + \sigma_z)$$

and:

$$\begin{cases}
(1-2\mu)\left[\Delta U - \frac{U}{r_m^2}\right] + \frac{\partial \varepsilon}{\partial r} = 0;\\
(1-2\mu)\Delta U + \frac{\partial \varepsilon}{\partial r} = 0
\end{cases}$$

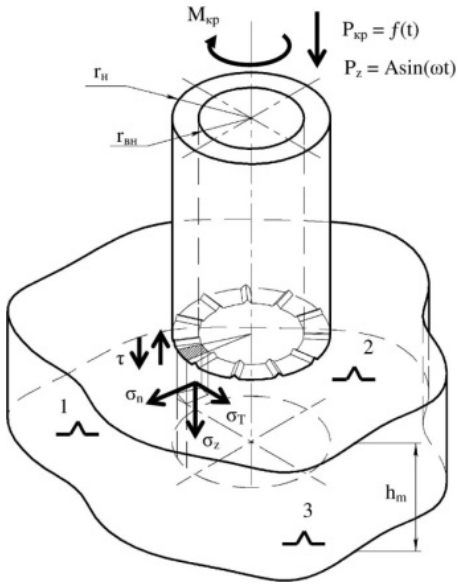

a)

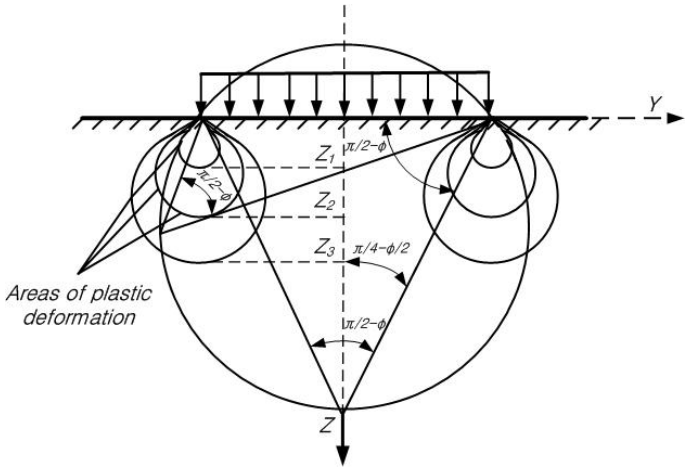

b)

Fig. 5. Drill action (a) and stress-strain state in the cutting zone (b)

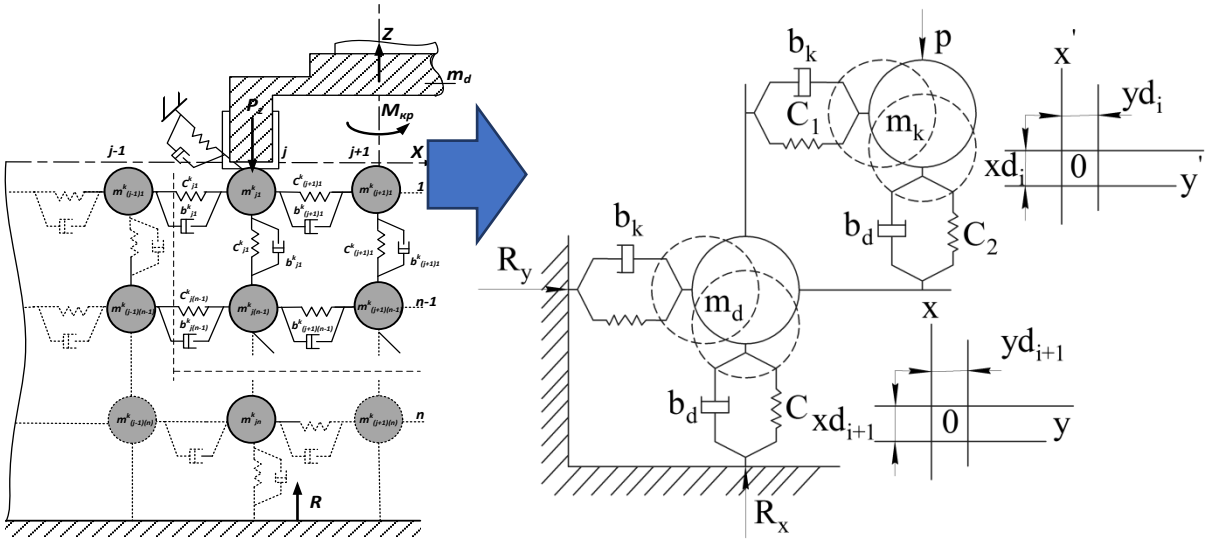

Fig. 6. Kinematic scheme of the impact on the cutting tool's cutting edge on the fiber

Table 3 *The Basic mechanical properties of carbon fibers [1]*

Characteristic	Carbon Fibers based on polyacrylonitrile			Carbon Fibers based liquid crystal pitch
	high strength	high elongation	highly modular	
Fiber diameter, nm	(7-9) 10^3	(6-7) 10^3	(6-9) 10^3	$1*10^5$
Tensile modulus, GPa	239-241	230-256	357-458	384-693
Tensile stress, GPa	3,0-3,5	4,0-4,5	2,0-2,5	2,1-2,4
Elongation at Tension,%	1,3-1,4	1,7-1,8	0,5-0,6	
Density, g / cm^3	1,74-1,78	1,74-1,78	1,78-1,84	2,00
Specific strength, m	173-196	230-252	112-146	105-120

Table 4 *The main technical characteristics of the fiber tow*

Linear Density (for CC CM)	350±50 (400±40) teks
Breaking load, H, not less	45
Bending strength in plastic, MPa, not less than	1078
Modulus of elasticity in bending in plastic, MPa, not less	127,4
Dynamic modulus of elasticity, GPa, not less	225
Effective processing temperature of the tow ^{0}C, not less	1900
Bulk density, g/cm^3, not less	1,68
Type of dressing	epoxy compatible
Twist, no more	15 m^{-1}
Linear density	текс

Therefore, for the ring effect we obtain the values of $U(t)$ and $H(t)$ fig.5b:

$$U(t) = -\frac{(1-2\mu)}{G}\frac{P_z(t)}{(D_{max}-D_{min})^2} r, r > \frac{D_{max}}{2}$$
$$H(t) = -\frac{(1-2\mu)}{G} P_z(t) \frac{2}{\pi(D_{max}-D_{min})}. \quad (8)$$

Here G – the shear modulus of the material being processed; μ – its Poisson's ratio; ε – the volume deformation; $\Delta = \frac{d^2}{dr^2} + \frac{d}{rdr} + \frac{d^2}{dz^2}$ – the Laplace operator.

The processed half space is not dense. This requires consideration of its dynamic properties. According to the concept of PSE, the material appears to be a layered structure (in the form of some kind of conjugated fibers), which generally exhibits quasi-brittle properties, with cores of elastic-plasticity on the bonds, that is, in the nodes of the polymer matrix presence.

Then the material processed becomes a medium with a periodically varying structure that can be perceived as an elastic-plastic compound of concentrated masses (according to the Kelvin-Voigt processed body model), for which the stress distribution between the components (fiber bundle and matrix) corresponds to the equation:

$$\sigma = E\varepsilon + \eta\frac{d\varepsilon}{dt}, \quad (9)$$

where E – the modulus of elasticity of the elastic component; η – the viscosity of the component of the medium (matrix).

The deformations ε will be $\varepsilon = \frac{\sigma}{E}\left(1 - e^{\frac{t}{\tau}}\right)$ the behavior of the PSE components will be described by the

corresponding differential equations. According to the scheme of fig. 6 the contact of the processed material with the tool and the bearing surface occurs with the occurrence of a cutting force F on the top layer and the reaction of the support R_x on the bottom in the vertical plane, and in the radial – as a balanced reaction to deformation of the surface with the drill. Then for the upper layer and for the normalized mass of the tool:

$$\begin{aligned} m_k \frac{d^2 x_k}{dt^2} - b_k \frac{dx_k}{dt} - c_1 x_k &= P; \\ m_d \frac{d^2 x_d}{dt^2} - b_d \frac{dx_d}{dt} - c_2 x_d &= -R_x; \\ m_k \frac{d^2 y_k}{dt^2} - b_k \frac{dy_k}{dt} - c_3 y_k &= \sigma_k f_k; \\ m_d \frac{d^2 y_d}{dt^2} + b_d \frac{dy_d}{dt} + c_4 y_d &= R_y. \end{aligned} \quad (10)$$

In this case, $R_x = \frac{c_1 c_2}{c_1 + c_2}\left(x_k + x_d\right)$,

$R_y = \frac{c_3 c_4}{c_3 + c_4}\left(y_k + y_d\right) = \sigma_k f_k$ and the movement of the components in the vertical plane will occur in accordance with the cyclic action of the axial feed.

For the intermediate layers, we have the following equations system.

$$\begin{aligned} m_{k(n-1)} \frac{d^2 x_{kn-1}}{dt^2} - b_{kn-1} \frac{dx_{kn-1}}{dt} - c_{kn-1} x_{kn-1} + b_{kn} \frac{dx_k}{dt} + c_{kn} x_{kn} &= 0; \\ m_{k(n-1)} \frac{d^2 y_{kn-1}}{dt^2} - b_{kn-1} \frac{dy_{kn-1}}{dt} - c_{kn-1} y_{kn-1} + b_{kn} \frac{dy_k}{dt} + c_{kn} y_{kn} &= 0. \end{aligned} \quad (11)$$

THE RESULTS

Below are the results of model experiments and studies of processing KIMF-type material during drilling with a cyclic feed. When modeling, the real structure of the simulated composite materials (Fig. 7a,b), the surface profile of the diamond tool (Fig. 7c) were taken into account, and the properties of individual fibers, as well as the properties of fiber bundles, are given in tables 3.4. Since the structure of the carbon-carbon material was 3-d weaving (and the studied plastic had a simpler satin weaving), the main attention was focused on it.

According to microphoto fig. 7, the geometric parameters of the PSE necessary for the calculations were also determined. It is established that the carbon fiber bundle represented by the PSE nucleus has a diameter of d_v 1,57–1,72 mm; the polymer matrix covers the bundle with a layer of s_{pp} 0,35–0,55 mm; the thickness of the intermediate layer with air cavities equals to s_{pv} 0,18–0,22 mm.

Separate diamond grains with a fraction of 150/200 microns are observed on the surface of the cutting edges of the tool (fig. 7b) separate diamond grains with a fraction of 150/200 microns are observed; the density of such grains arrangement is 250–300 u/cm^2.

The TL–90 type profilometer was used to determine the grain reach value. As a result of elaboration, it is established that the particles protrude above the surface at a height of 0,08–0,68 mm.

The calculation of the expected magnitude of the particles to be produced during the processing indicates (fig. 8) that in the sludge, the particles of the polymer matrix, the broken fibers and the conglomerates for which the cracks have developed to a critical size can be separated.

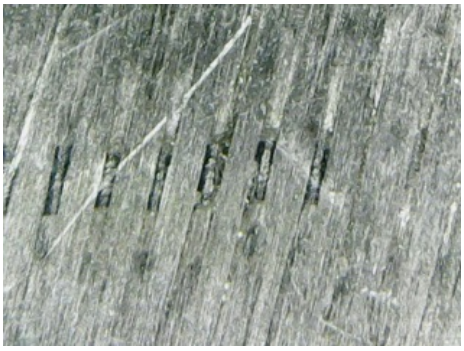

a)

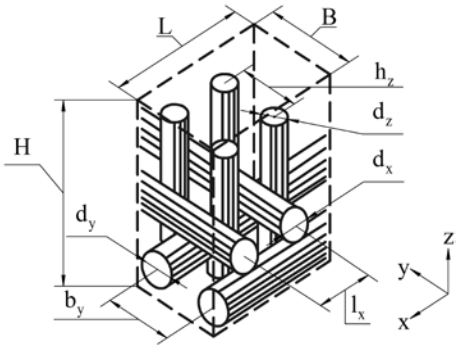

b)

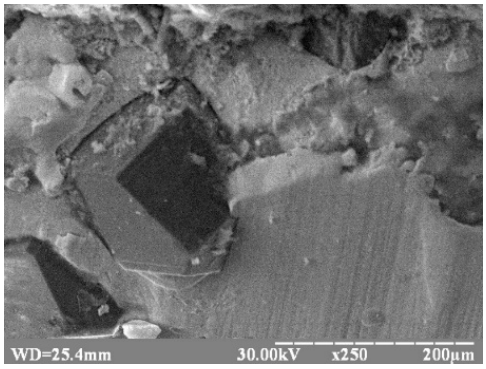

c)

Fig. 7. Microphotos of the carbon materials (a), structure (b) and the surface of a diamond-coated tubular drill (c)

It is easy to see that the characteristic particle size (for example, length l_z or larger size) is due to:

1) Orientation of the reinforcing fibers relative to the applied force (since E and G components change, with changes in σ ; (4);

2) The size of the protruding abrasive grains, according (6) (varies l_i and σ ((fig. 8);

3) Frequency of variable axial load n, N and, accordingly, M_f (5).

The stresses in the surface layer σ_0, caused by the force of the axial feed P.

The analysis of the results of the calculations proves that all the factors taken into account are valid, though having different degrees of influence. The most significant influence on the size of the sludge particles has a forceful effect on the material to be processed (fig. 8). It can be expected that an increase in the applied axial force will cause a corresponding increase in stresses at the contact surface and that individual fibers and their conglomerates will be cleft. From the diagram above (fig. 8), it can be seen that a stress exceeding 40 MPa significantly increases the size of the sludge particles; and based on the physical model of surface formation with a single grain, an inference can be made that the roughness will increase on the surface.

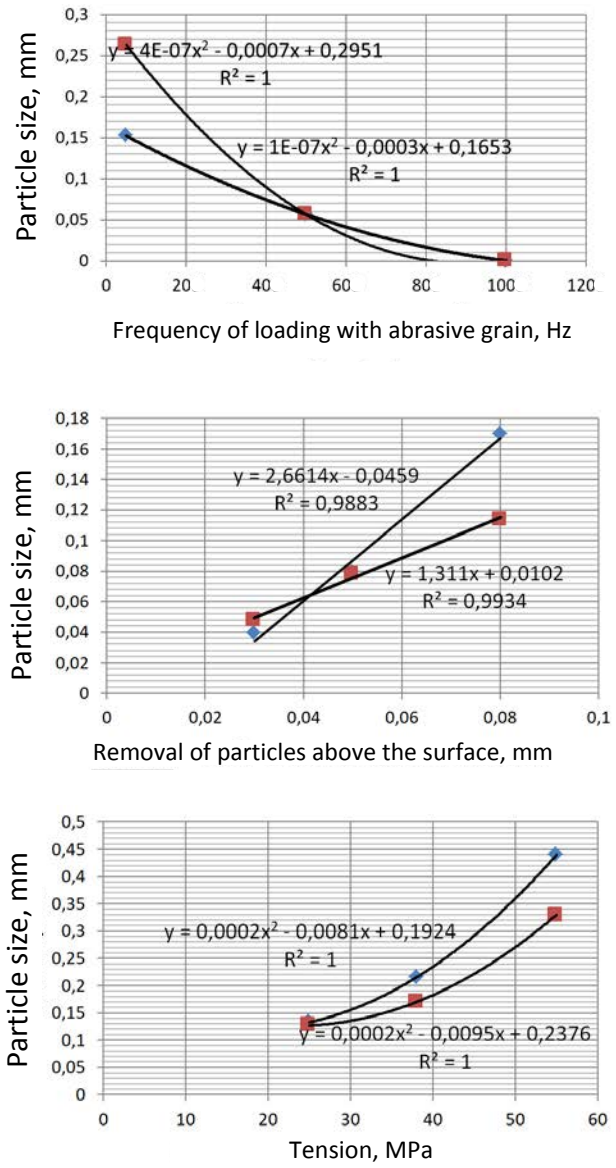

Fig. 8. Change in the expected size of the sludge particles depending on the conditions of interaction with the material, which is represented as an assumed PSE with different fiber orientation

The influence of fiber orientation on the sludge fraction is not significant within the stresses of 15–40 MPa; orientation of fibers at angles approaching $\pi/4$ leads to a decrease in the sludge fraction by 20…35%. The frequency of the working tool oscillation influences the size of the sludge particles significantly.

The use of low-frequency loading of the working body edge (in the frequency range 50–100 Hz) causes the appearance of significant sludge particles, the characteristic size of which can be expected at the level of 0,18–0,27 mm. Since the frequency has the reverse effect, and the fiber bundles can significantly loosen without a matrix, such particles can be formed mainly from an adhesive.

The impact of the size of the console of the protruding part abrasive virtually linearly changes the expected sludge fraction: reduction in the reach value to 0,08 mm alters the microstress in the tip and affects the development of the microcrack mesh. Cracks begin to grow more actively, with particle size formation up to 0,08–0,12 mm. In this case, the sludge contains separate fractions of cut carbon fibers and polymer matrix (fig. 9).

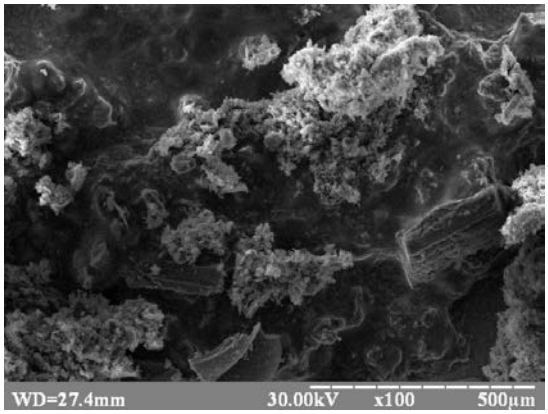

Figure 9 – Conglomerates of fibers and fine sludge from adhesive residue

Now, having an idea of the structure of the composite as an aggregate of PSE, let us solve the given system of equations with respect to $U(t)$ and $H(t)$ and establish the difference $P = (U(t) - y_k(t))$, for different layers of material. Note, that the thickness of the layer formally corresponds to the size $h^s = d_v + 2s_{pp} + 2s_{pv}$.

We can see, that the stresses on adjacent elements are found under the condition of greater (I) and lesser (II) hollowness (fig. 10).

The presence of horizontal displacements between the coupled PSE on the layer following the plane of force application can be considered the stratification condition. Then PSE stresses values will be caused by position of the processed workpiece blank in accordance with fig. 9, whereas PSE parameters, will determine the level of stresses under, taking into account the structure hollowness (in fig. 10 the results of σ_i change are provided as ratio of dynamic forces in elements to PSE contact area, which is determined by its geometry).

To determine the dynamic parameters of model c and b, we take into account that under the action of the axial force, deformations occur on the contact plane, which are capable of causing adhesion disturbances in the intercontact space. In this case, the reinforcing fibers are excluded from the material, and the characteristics of c and b correspond to the properties of the polymer matrix.

The fiber exclusion length at destruction is determined, [5]:

$$l_0 = \frac{\sigma_{fb} - \sigma_{f\tau}}{13\sqrt{b'E k_\tau \tau_\tau}} l_c,$$

where b' – the crack depth; l_c – the crack length; E – modulus of elasticity; τ_τ – tangential stresses;

$k_\tau = 0{,}3...1{,}5$. The parameters indicated are determined by the micromechanics of the material, i.e. the characteristics of the interaction of grain with the surface.

Thus, if $U(t)$ exceeds the value of $y_k(t)$ with the occurrence of the corresponding stresses, which, taking into account the assumed assumptions with respect to PSE, will be:

$$\tau = G\left(\frac{\partial U((t)-y_k(t))}{\partial r} + \frac{\mu\varepsilon}{1-2\mu}\right),$$

there will be an internal delamination of the material outside the applied force area.

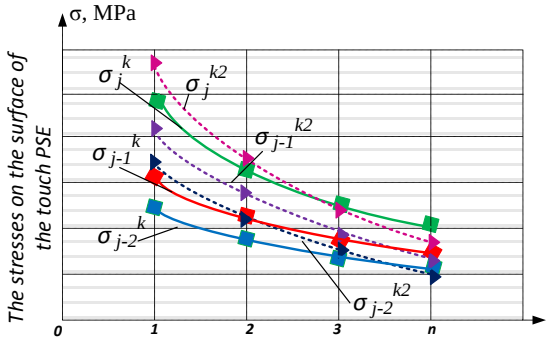

σ^{k} - tensions options at PSE group I

σ^{k2} - tensions options at PSE group II

Fig. 10. Distribution of stresses in the PSE depending on their location relative to the applied cutting force

We take the harmonic law of force F_z change as the acting load: $F_z = Asin(\omega t)$. The changes in the intersection stresses τ are shown in fig. 10. Each layer is indicated by a line $y1 - y3$ in the scan for the time axis t_i .

In fig. 11-13 the results of modeling the influence of the form of oscillations and the frequency of oscillations of the tool end on the magnitude and shape of the stresses arising on the first plane are provided. The impact is given as a single full-period effect at time *T*, *T*=0,02 s. The damping of the bonds is neglected, but the rheological properties of the composite components were taken into account.

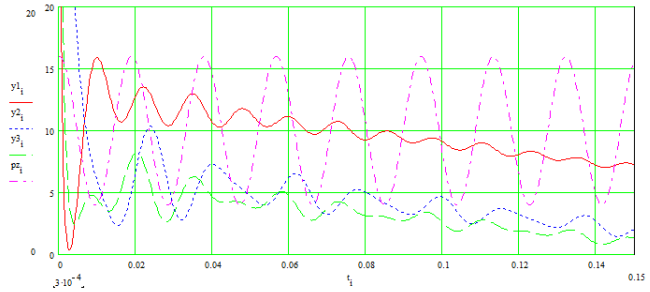

Fig. 11. The stresses that arise between the layers of composite material when applying periodic load (complies with the law pz1): $y1_i$ – after the first layer; $y2_i$ – after the second; $y3_i$ – after the third one

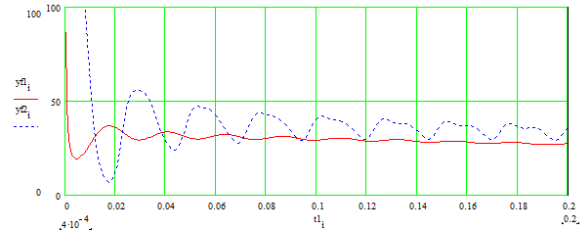

Fig. 12. Change of stresses at different forms of oscillation of the cutting tool end yf_1 – harmonic shape; yf_2 – impact-dynamic

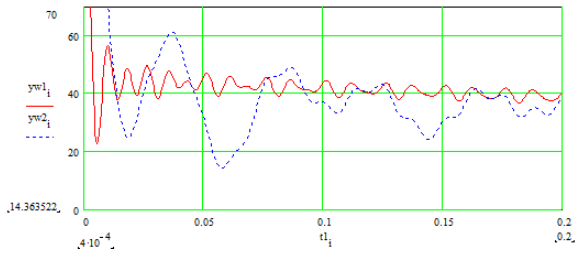

Fig. 12. Effect of oscillation frequency on the change of tangent stresses on the adhesion surface: increasing the frequency above 80 Hz leads to a significant decrease in the amplitude of the stresses arising

Several conclusions can be drawn from the following diagrams.

The application of oscillations influences the stresses arising on the adhesion planes of the components of the composite significantly (reinforcing carbon fibers and polymer matrix). Thus, fig. 11 compares the forms of stress fluctuations on the first surface following the action plane when the shock-dynamic (yf_2) and harmonic (yf_1) effects are applied. Impact-dynamic impact corresponds to a sawtooth-like load with sharp increase in axial force and smooth unloading. In this case, it is obvious that the damping of such oscillations occurs slower, that is, it can be expected that the destruction of the material will occur in accordance with the scheme of low-cycle loading.

The tangential stresses decrease the penetration of the material, their phasal nature is changed, which generally corresponds to the accepted assumptions when modeling the PSE composite. The maximum stress values are observed on the first layer following plane of reinforcement fibers separation. At the expected level of stresses due to the quasi-static force P_z action and stresses emerging on the contact plane at the level of 20 MPa, on the stress layer following the surface, will reach 15 MPa. At the same time, increasing the frequency of the tool end oscillations over 80 Hz leads to a decrease in the amplitude of stresses in the interlayer intervals (fig. 12) from almost 40 MPa (at 40–50 Hz) to 10 MPa (at 90 Hz).

The distortion of the oscillation shape is due to the dissipative component and the nonlinearity taken into account, which is related to the exclusion of fibers at stresses exceeding 30 MPa (fig. 11, 12).

Consequently, the material should be processed in a cyclically variable feed, but provided that there is no impact on the cutting zone.

PRACTICE USING

Overlapping of the corresponding vibrations on the working tool (due to cyclic linear feed) greatly increases the drilling efficiency. To provide this movement (supply with oscillatory displacement of the ends), a technical solution is proposed for a power drive with connected electric machines [13], [14].

The schematic diagram of the device – the spindle node is shown in fig. 13. The assembly consists of a housing 1, which, on the one hand, with the possibility of longitudinal motion along the central axis, mounted a pin 2, fixed from the possible rotation of the pin 3, which is in contact with the rectilinear guide groove 4, located on the housing 1.

The moving stroke 7 of the main motion electric motor with a winding of 7 is mounted on the moving pin 2 with the terminals for supplying the voltage 6 so that the axes of

the piston 2 and the windings 5 coincide. In the inner cavity of the pencil 2, a motionless stator 5 of the flow feeder with a winding 7a with terminals for supplying voltage 8, inside of which a rotor 9 is installed, is fixedly connected to the spindle 10, made in the form of a shaft, one of the ends of which has a flange for fastening the tool 11, and on the other end a screw surface 12 is provided. To provide a rotational motion, the spindle 10 is mounted on the thrust-radial supports (bearings) 13 and 14, mounted in the pin 2.

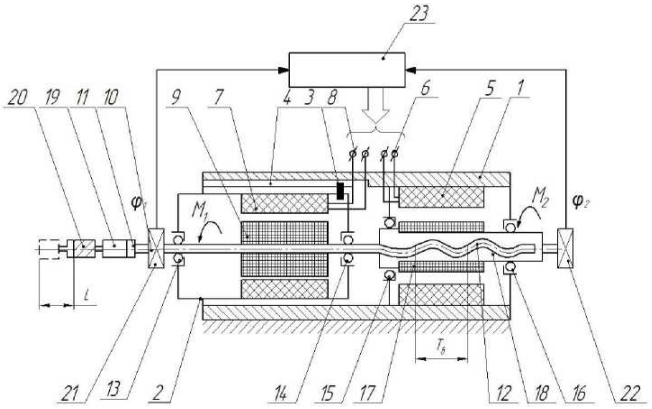

Fig. 13. Principle diagram of the power head

Concentrically to the stator 7 in the radial tensile pins 15 and 16 mounted in the body 1, a rotor 17 is located fixedly connected to the nut 18, with the axis of the rotors 17 and 9 and, accordingly, the spindle 10 and the nuts 18 coincide, and the screw surface 12 of the spindle 10 is connected to the screw surface of the nut 18, forming a mobile screw-nut type with it.

The flange 19 is mounted on the flange 11, in which the tool 20 is secured. With the output end of the spindle 10 and the end of the nut 18, the sensors of the angles of turns 21 and 22 are connected, which, in turn, are connected to the control system 23 and control the angles the rotation φ_1 of the spindle 10 and φ_2 of the coupling 18. The control system 23 is connected to the output circuits with terminals 6 and 8, and together with the sensors of angular positions 21 and 22 forms a closed electromechanical circuit.

Such a combination of a housing with a movable spindle and a clamping device, a veneer located in the front of the body, a stator of an electric main machine, a spindle with a distributed winding, fixed inside the vane, a rotor rigidly connected to the spindle, and an electric drive in the form of an additional stator An electric machine coupled to the body and mounted in a coil of the spindle and the rotor, which interacts through the «screw-nut» connection with the spool, makes it possible to perform the flow of motion in the event of a difference in angular velocity Awning two rotors, which is controlled by the appropriate control system. In this case, the coaxial performance of the electric drive frees the spindle and allows you to balance the feedstock during drilling; the absence of extra gear and other gear increases the accuracy and stability of the system.

For verification of the formulated provisions, the simulation, fabrication and testing of combined electric machines, performed on the principle of stepping motors, was carried out. The system of differential equations is given below.

$$J_R\frac{d^2\varphi_1}{dt^2}=M_e^I-M_k-M_{01}-C_1(\varphi_n-\varphi_1)-b_1\left(\frac{d\varphi_n}{dt}-\frac{d\varphi_1}{dt}\right)$$

$$J_0\frac{d^2\varphi_n}{dt^2}=C_1(\varphi_n-\varphi_1)-b_1\left(\frac{d\varphi_n}{dt}-\frac{d\varphi_2}{dt}\right)-M_{fr}-C_1(\varphi_2-\varphi_n)-b_2\left(\frac{d\varphi_2}{dt}-\frac{d\varphi_n}{dt}\right)$$

$$J_2\frac{d^2\varphi_2}{dt^2}=M_e^{II}-M_{02}+C_2(\varphi_2-\varphi_n)-b_2\left(\frac{d\varphi_2}{dt}-\frac{d\varphi_n}{dt}\right)$$

$$\frac{d\varphi_1}{dt}=\omega_1;\ \frac{d\varphi_2}{dt}=\omega_2;$$

$$m_1\frac{d^2Z}{dt^2}=-P_z+C_3k(\varphi_2-\varphi_1)-b_3k\left(\frac{d\varphi_2}{dt}-\frac{d\varphi_1}{dt}\right);\ \frac{dz}{dt}=v_z,$$

where φ_1, φ_n, φ_2 – respectively the absolute angles of rotation of the spindle, coupling, and rotor of the second electric machine and the moment of inertial damper; C_1, C_2, C_3, b_1, b_2, b_3 – dynamic coefficients of the mathematical model; M_{fr} – moment of friction, M_k – the moment of the kinematic chain between the motor shaft and the coupling; M_{01}, M_{02} – the total torque of the nut resistance; M_e – the moment of electromagnetic forces acting on the rotor.

The electromagnetic processes in the motors were described by known regularities, which are not given here due to the limited volume.

By the work of connected electric machines, control pulses were set so that at corresponding rotation of the output end of the spindle ϕ_i and linear axial feed θ_i, and with a fixed base on the surface of the treatment, corresponding loads appeared in accordance with fig. 14.

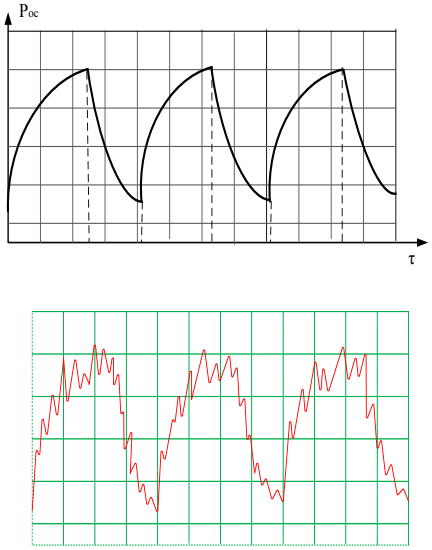

Fig. 14. Cyclically variable load of the working tool during drilling

The special equipment for the drilling and drill that used given on fig.15; and transients are shown in fig. 16. Main characteristics of Carbon-Carbon Composite Materials given on table 5.

Since, in the process of drilling a material, which is long fiber reinforcing carbon fiber and pyro carbonate layers, it is converted into fine particle dust of sufficiently small fractionality. Divided into a gap between the formed surface of the treatment and protruding diamond grains, the dust under the action of a number of forces begins to move. In this case, the adhesive properties, aerodynamic, contact

interaction between the particles and the surface, as well as the inertial forces are manifested. The dust particles stick to the surface, changing the height of the abrasive grain leaving and changing the spot of the dynamic contact between the tool and the material being processed.

A detailed physical description of the phenomena in the cutting zone allowed to perform the mathematical modeling of dust formation and to obtain the regularities of the change in the intensity of the dusting of I_i (and, accordingly, the concentration of dust particles in the K_i) in the gap between the tool base and the surface to be processed.

Comparison of controlled indicators has proven that a more stable and long-lasting treatment with a low frequency (up to 50 Hz) fluctuations and a certain law of motion of the end of the instrument.

The results of processing with cyclic feed and without feed are shown in table 6. From the above results, it becomes obvious that the most appropriate load for drilling is a cyclic-variable load, which allows the highest quality of the hole (fig.17). Other indicators are shown in fig. 18–20.

a)

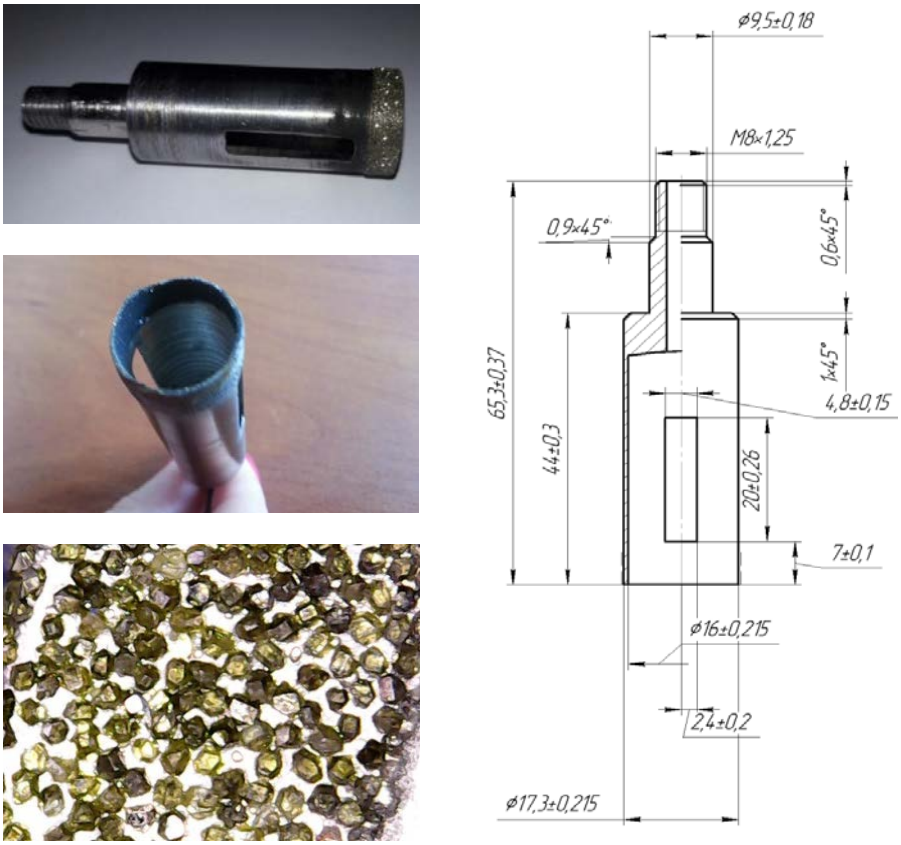

b)

Fig. 15. Special equipment for the drilling (a), drill that used and it geometric parameters (b)

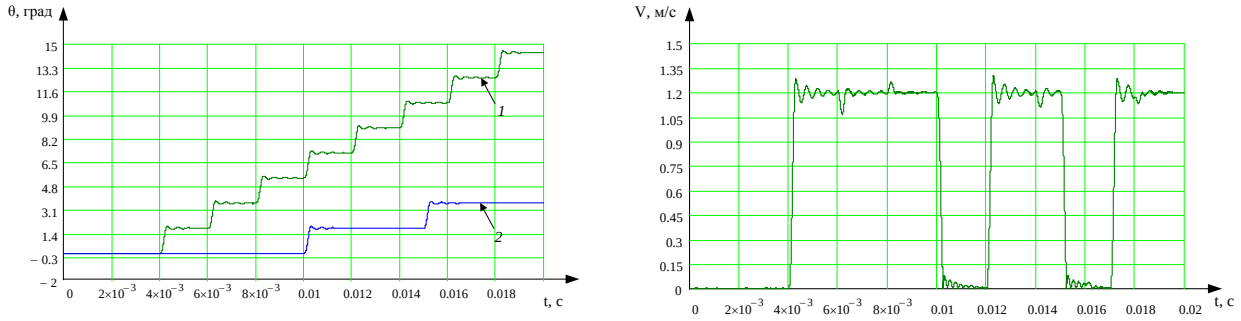

Figure 16 – Rotation angle of stepper motors: 1 – main drive actuator 2 – feed motion actuator

Table 5 *Main characteristics of Carbon-Carbon Composite Materials*

Bulk (apparent) density, not less than, g/cm^3	1,7
Breaking stress kg/cm^3 during compression along the axes of reinforcement X (Y), not less	1200
Breaking stress kg / cm^3 during tension along the axes of reinforcement X (Y), not less than	240
Breaking stress during shear, MPa, not less	24,5
Breaking stress at bending, MPa, not less	88,2
The coefficient of thermal conductivity (at a temperature of 50° C), kcal/m hour, deg	7
Modulus of elasticity in compression along the axes of reinforcement X (Y), MPa, not more than	2,45·10^4
The porosity of the material,%	*8,7
Impact strength, kJ/m^3	*10
Electrical resistivity, Ohm· mm^2/m	30

Table 6 *Comparison of the cyclic feed effect created by the proposed power head, when forming the hole surface*

№	*Conditions*	*Surface microphoto*	*Form of change of workload*	*Characteristics*
1	D_{dr}=8 mm; ω=3000 rpm; frequency= 40 Hz.		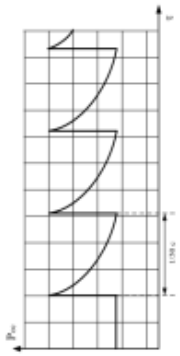	Tearing the fibers, loosening the edges
2	D_{dr}=8 mm; ω=3000 rpm; frequency= 70 Hz.			Loosening edges
3	D_{dr}=8 mm; ω=3000 rpm; frequency=35 Hz.		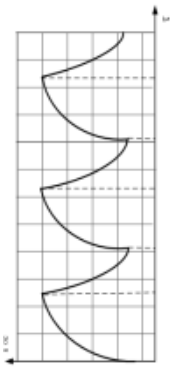	Satisfactory hole quality R_a=6,3
4	D_{dr}=8 mm; ω=3000 rpm; frequency= 40 Hz.			Increased roughness R_a=6,5…12
5	D_{dr}=8 mm; ω=3000 rpm.		Without cyclic loading	Significant defective layer δ=0,15 mm

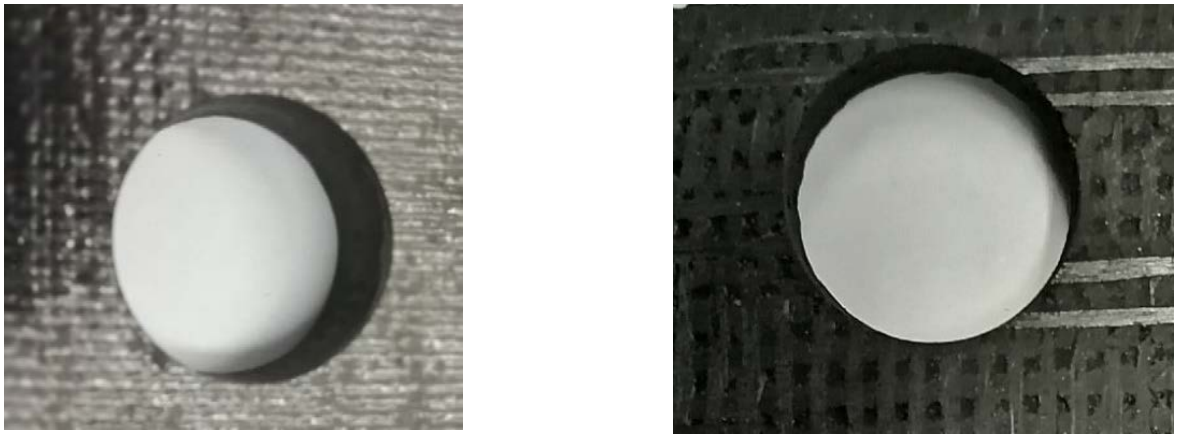

a) *b)*

Fig. 17. Examples of hole in carbon plastic (a) and carbon-carbon composite material (b)

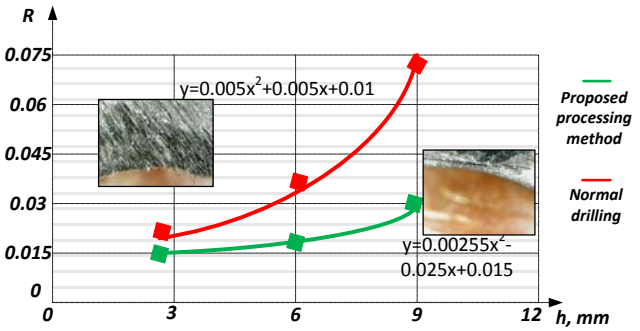

Fig. 18. The results of surface layer quality studies (destruction level) after processing

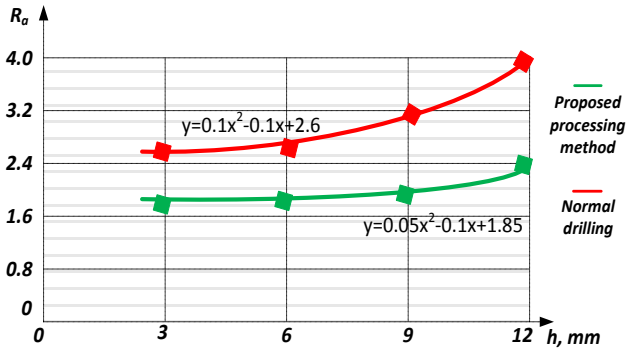

Fig. 19. Results of surface layer roughness studies after processing

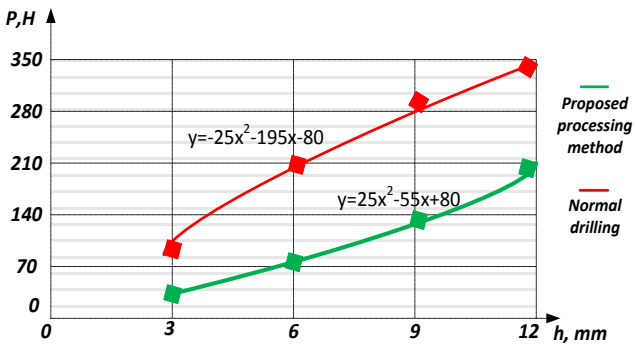

Fig. 20. Results of drilling effort studies

Thus, the use of PSE approaches made it possible to describe the interaction of diamond grains with a porous surface and to determine the characteristic particle size depending on the orientation of the reinforcing fibers with respect to the applied force; the size of the protruding particle of the abrasive grains, the frequency of alternating axial loading and the stresses in the surface layer σ_0, due to the force of the axial feed P. The influence of fiber orientation on the sludge fraction is not significant within the stresses of 15 - 40 MPa; orientation of fibers at angles approaching $\pi/4$ leads to a decrease in the sludge fraction by 20… 35%. The frequency of oscillations of the working tool has a significant influence on the particle size of the sludge: oscillations in the frequency range of 40-600 Hz lead to the appearance of finely dispersed sludge, since the cracks cease to develop and bifurcate with the formation of finely dispersed particles, and the low-frequency range 100 Hz) causes the appearance of quite significant sludge particles, the characteristic size of which can be expected at the level of 0.18-0.27 mm. The impact of the size of the console protruding part of the abrasive almost linearly changes the expected sludge fraction: reducing the departure to 0.08 mm alters the microtension in the tip and affects the development of the network of microcracks. Cracks begin to grow more actively, with particle sizes of 0.08-0.12 mm.

Consideration of the material from the point of view of macromechanics has proved that the axial force load of the cutting zone causes the appearance of tangential stresses at the interlayer intervals, which can lead to material delamination. The shear stresses decrease the depth of the material, their phase is changed, which generally corresponds to the accepted assumptions when modeling the PSE composite. The maximum stress values are observed on the first layer of reinforcement layer from the separation plane. At the expected level of stresses from the quasi-static action of the feed force and the occurrence of stresses on the contact plane at the level of 20 MPa, at the first from the surface the stress layers will reach 15 MPa. At the same time, increasing the oscillation frequency of the tool end more than 80 Hz leads to a decrease in the amplitude of the stresses between the layer intervals from almost 40 MPa (at a frequency of 40-50 Hz) to 10 MPa (at a frequency of 90 Hz).

An original technical solution is proposed - a spindle motor with coupled electric machines, which provides

rational linear-rotary movement of the tool to ensure rational processing conditions.

CONCLUSIONS

As a consequence of the performed set of theoretical and experimental research, the stress state of the cutting zone in composite materials based on carbon fibers has been evaluated and it is proved that their processing with ring diamond-coated drills is reasonable and effective. The use of a cyclic linear feeder allows significantly reducing the thickness of the destructive layer and reducing the cutting force, requiring further research on the issue of rational geometric dimensions of the tool end, the presence of cavity elements on it to remove the microstrip from the processing area.

It is also proven that the proposed design of a power head with coupled electric machines to provide rotary and translatory motion in coaxial execution is a promising technical solution that can be successfully implemented in both manual tools and automated processing programmed control systems.

REFERENCES

[1] Kerber M.L., Polimernyye kompozitsionnyye materialy. Struktura. Svoystva. Tekhnologii. SPb.: Professiya, 2008

[2] Verezub N.V. Energeticheskiye aspekty razrusheniya polimernykh kompozitov pri rezanii / N.V. Verezub, G.L. Khavin, A.P. Tarasyuk // Rezaniye i instrument v tekhnologicheskikh sistemakh. Mezhd. nauch.-tekhnich. sb. – Kharkív: NTU«KHPI», 2001. – №59. – S. 28–34.

[3] Bondarenko, G.A., Penkin N.S. Osobennosti geometrii sverl dlya obrabotki polimernykh materialov / G.A. Bondarenko, N.S. Penkin // Sbornik nauchnykh trudov SevKavGTU, seriya «Yestestvennonauchnaya», №2, 2006. – s. 115-117.

[4] Sheikh-Ahmad J., Paulo Davim J. Cutting And Machining of polymer Composites, Wiley Encyclopedia of Composites, 2012.

[5] Xu J, Li Xi, Chen M, El Mansory M, Ren F. Study of the drilling process of high-strength carbon composite materials using specialized drills. Int J Adv Manuf Technol 2019; 103 (9): 3425-42.

[6] Xu J, Li Si, Dang J, El Mansory M, Ren F. Study of drilling high-strength carbon fiber laminates: friction temperature and cutting temperature. Materials 2018; 11 (12): 2366.

[7] Xu J, An Q, Cai X, Chen M. Assessment of machinability for drilling on new high-strength carbon fiber laminates T800S / 250F. Int J Precis Eng Manuf 2013; 14 (10): 1687-96.

[8] Xu J, Li C, Mi S, An Q, Chen M. Investigation of defects caused by drilling for carbon fiber composites using new criteria. Compos Struct 2018; 201: 1076-87.

[9] Kirichenko A., Metaq Al Ibrahim, Schetinin V., Chencheva O. ″Improving the quality of abrasive cutting carbon-carbon composites through rational conditions of dynamic contact″, Transactions of Kremenchuk Mykhailo Ostrohradskyi National University, vol. 5 (112), pp. 94–102, 2018.

[10] Wang H., Sun J. and et. ″Evaluation of cutting force and cutting temperature in milling carbon fiber-reinforced polymer composites″, International Journal of Advanced Manufacturing Technologies, vol. 85, pp. 9–12, 2015.

[11] Xu J, El Mansori M. Experimental studies of the cutting performance of hybrid CFRP / Ti stacks. Manuf Procedure 2016; 5: 270-81

[12] Salenko A., Chencheva O., Lashko E., Shchetynin V., Klimenko S., Samusenko A., Potapov A., Gusarova I. ″Forming a defective surface layer when cutting parts made from carbon-carbon and carbon-polymeric composites″, Eastern-european journal of enterprise technologies. Engineering technological systems 4 (1) (94) 62–73, 2018

[13] Salenko A., Chencheva O., ″About expediency of the use of combined rotating electric cars in power heads of new technological equipment″, Transactions of Kremenchuk Mykhailo Ostrohradskyi National University 4 (87) 111–119 2014.

[14] Kuznietsov Y., Shinkarenko V. "The Genetic approach is the key to innovative Synthesis of complicated Technical Systems" Journal of the Technical University at Plovdiv, Bulgaria Fundamental Sciences and Applications, 16 (2011) 15–33